





Article

Anti-Inflammatory Constituents of *Antrodia camphorata* on RAW 264.7 Cells Induced by Polyinosinic-Polycytidylic Acid

Ping-Chen Tu ^{1,2} , Wen-Ping Jiang ², Ming-Kuem Lin ¹ , Guan-Jhong Huang ^{1,3} , Yi-Jen Li ⁴
and Yueh-Hsiung Kuo ^{1,5,6,*} 

¹ Department of Chinese Pharmaceutical Sciences and Chinese Medicine Resources, China Medical University, Taichung 40402, Taiwan

² Department of Pharmacy, Chia Nan University of Pharmacy and Science, Tainan 71710, Taiwan

³ Department of Food Nutrition and Healthy Biotechnology, Asia University, Taichung 413, Taiwan

⁴ Department of Nutrition and Health Sciences, Chang Jung Christian University, Tainan 71101, Taiwan

⁵ Department of Biotechnology, Asia University, Taichung 41354, Taiwan

⁶ Chinese Medicine Research Center, China Medical University, Taichung 40402, Taiwan

* Correspondence: kuoyh@mail.cmu.edu.tw; Tel.: +886-4-2205-3366 (ext. 5709)

Abstract: *Antrodia camphorata* is an endemic mushroom in Taiwan. This study was designed to screen anti-inflammatory compounds from the methanolic extract of the mycelium of *A. camphorata* on nitric oxide (NO) production in RAW 264.7 cells induced by polyinosinic-polycytidylic acid (poly I:C), a synthetic analog of double-stranded RNA (dsRNA) known to be present in viral infection. A combination of bioactivity-guided isolation with an NMR-based identification led to the isolation of 4-acetylanthroquinol B (**1**), along with seven compounds. The structure of new compounds (**4** and **5**) was elucidated by spectroscopic experiments, including MS, IR, and NMR analysis. The anti-inflammatory activity of all isolated compounds was assessed at non-cytotoxic concentrations. 4-Acetylanthroquinol B (**1**) was the most potent compound against poly I:C-induced NO production in RAW 264.7 cells with an IC₅₀ value of 0.57 ± 0.06 μM.

Keywords: *Antrodia camphorata*; 4-acetylanthroquinol B; RAW 264.7 cells; poly I:C



Citation: Tu, P.-C.; Jiang, W.-P.; Lin, M.-K.; Huang, G.-J.; Li, Y.-J.; Kuo, Y.-H. Anti-Inflammatory

Constituents of *Antrodia camphorata* on RAW 264.7 Cells Induced by Polyinosinic-Polycytidylic Acid.

Molecules **2022**, *27*, 5320. <https://doi.org/10.3390/molecules27165320>

Academic Editor: Diego Muñoz-Torrero

Received: 6 July 2022

Accepted: 15 August 2022

Published: 20 August 2022

Publisher's Note: MDPI stays neutral with regard to jurisdictional claims in published maps and institutional affiliations.



Copyright: © 2022 by the authors. Licensee MDPI, Basel, Switzerland. This article is an open access article distributed under the terms and conditions of the Creative Commons Attribution (CC BY) license (<https://creativecommons.org/licenses/by/4.0/>).

1. Introduction

Inflammation is part of the innate, or nonspecific, immune responses against invading pathogens. It is generally initiated when pathogen-associated molecular patterns (PAMPs), such as pathogen-specific carbohydrates, lipoproteins, and nucleic acids, are recognized by a large family of pattern-recognition receptors (PRRs), expressed by macrophages, monocytes, dendritic cells, and neutrophils [1]. Among these immune cells, macrophages play a crucial role in inflammatory reaction through producing inflammatory factors, such as reactive oxygen species (ROS), nitric oxide (NO), cytokines, chemokines, and prostaglandins [2,3].

Notable outbreaks in the last two decades mostly involved respiratory viruses—such as the 2003 severe acute respiratory syndrome (SARS) epidemic, 2009 A(H1N1) pandemic, Middle Eastern respiratory syndrome (MERS) epidemic, and ongoing coronavirus disease 2019 (COVID-19) pandemic—that represent a considerable challenge to worldwide public health [4]. Novel respiratory viruses commonly lead to severe respiratory tract infections. Owing to the involvement of inflammatory signaling pathways in imbalanced host immune response, which cause acute lung injury in respiratory virus infection, mounting evidence points to the therapeutic potential of targeting viral induced-inflammation [5–7].

Plants are generally considered a rich source of natural products that can prevent the onset of diseases and reduce health care costs. A variety of natural products, including flavonoids, terpenoids, alkaloids, glycosides, quinones, and phenolic compounds, from plants traditionally used as antiviral agents have been reported to possess remarkable

potential against viral infection [8–10]. Among them, anti-inflammatory phytochemicals have attracted much attention to providing potential therapeutic interventions in combating viruses and related complications [11]. *Antrodia camphorata* is an edible and precious mushroom endemic to Taiwan, which has been used as traditional medicine. *A. camphorata* has been found to exhibit a broad range of pharmacological effects, which include anti-microbial, anti-oxidative, anti-inflammatory, anti-diabetic, anti-aging, anti-carcinogenic, neuroprotective, hepatoprotective, cardioprotective, and immunomodulatory effects [12–15]. Phytochemical investigation of *A. camphorata* led to the isolation and characterization of diverse bioactive phytochemicals that include benzenoids, ubiquinones, maleic anhydride and maleimide derivatives, terpenoids, and steroids [12–15]. Anticins, unique steroid-like compounds isolated from *A. camphorata*, were reported to be novel anti-angiotensin-converting enzyme 2 (ACE2) agents for prophylaxis of COVID-19 [16]. Whether anti-inflammatory phytochemicals from *A. camphorata* show potency against inflammation in viral infection remains to be fully elucidated.

Recently, metabolomics can provide a rapid tool by allowing mixture analysis and simultaneously detecting diverse phytochemicals without the need for time-consuming chromatographic procedures. NMR-based identification is extremely powerful for rapid identification of natural products with relative concentration determination. Furthermore, relating metabolites with bioactivities is feasible by integrating metabolite profiling with bioassay results [17,18]. In this study, we combined an NMR-based identification approach with an anti-inflammatory assay to select natural products with inhibitory effects on NO production in RAW 264.7 cells induced by poly I:C, a synthetic analog of dsRNA known to be produced by viral replication and presented in viral infection.

2. Results and Discussion

Viral infections might provoke hyper-inflammation responses in macrophages. dsRNAs are produced by viral replication during viral infections and recognized by PPR [19]. As a synthetic analog of dsRNA, poly I:C was used to mimic the viral infection model both in vivo and in vitro in previous studies [19–21].

The inhibitory effects of the mycelium of *A. camphorata* on viral infection-associated inflammation have not been studied previously. Here, poly I:C was applied to stimulate NO production in a RAW 264.7 mouse macrophage cell line as a virus-induced inflammation model for investigating the anti-inflammatory effects of *A. camphorata*. As shown in Figure S1, the methanolic extract of *A. camphorata* mycelium (ACM) showed significant inhibition activity against excessive NO production in poly I:C-induced RAW 264.7 cells. The percentages of inhibition of NO production treated with ACM at concentrations of 5, 10, 20, and 40 $\mu\text{g}/\text{mL}$ were 53.39 ± 4.87 , 67.83 ± 5.74 , 84.35 ± 1.51 , and $90.15 \pm 1.33\%$, respectively. The methanolic extract of *A. camphorata* mycelium was then subjected to MPLC separation, and each of the collected fractions was assigned to one of ten main fractions based on TLC characterization. Fraction 5 potently inhibited NO production with percentages of inhibition of 42.00 ± 2.86 , 51.46 ± 5.62 , 69.05 ± 6.25 , and $78.58 \pm 3.68\%$ at concentrations of 1, 2, 5, and 10 $\mu\text{g}/\text{mL}$, respectively. Thus, Fraction 5 was chosen for further analysis.

The ^1H NMR experiment offers metabolite profiling, achieved by chemical shifts, J -couplings, and signal area integration. Particularly, the intensity of the signal in ^1H NMR spectra is proportional to the relative number of (equivalent) protons that give rise to the signal and thus could provide quantitative information about the different compounds in the mixture. Relating putative bioactivities with these metabolites is feasible by integrating metabolite profiling with bioactivity results. According to the inspection of ^1H NMR spectra, the presence of 4-acetylanthroquinol B (**1**) in Fraction 5 was deduced from the characteristic signals as follows: A highly deshielded proton signal at δ_{H} 5.72 (1H, d, $J = 3.2$ Hz) assigned as H-4; two olefinic proton signals at δ_{H} 5.21 and 5.11 (1H each, t , $J = 7.0$ Hz); an oxygenated proton signal at δ_{H} 4.62 (1H, m) assigned as H-15; two methoxy proton signals at δ_{H} 4.00 and 3.67 (3H each, s); acetyl proton signal at δ_{H} 2.09 (3H, s); two methyl proton singlets at

δ_{H} 1.65 and 1.55 (3H each, s); and one methyl proton doublet at δ_{H} 1.19 (3H, d, $J = 7.3$ Hz). The remaining methyl proton doublet at δ_{H} 1.26 was overlapped. The relative abundance of different compounds in Fraction 5 obtained by comparing the signal intensity in the ^1H NMR spectrum (Figure 1) then indicated that the anti-inflammation activity might be contributed to by the presence of 4-acetylanthroquinol B (1), which is a natural ubiquinone analogue isolated from the mycelium of *A. camphorata* in 2009 [22]. As one of the bioactive compounds in *A. camphorata*, it has been reported to possess various bioactivities, which include anti-inflammatory, anti-carcinogenic, hepatoprotective, and immunomodulatory properties [22–28]. However, the role of 4-acetylanthroquinol B (1) in a viral-induced inflammation model has not been reported previously.

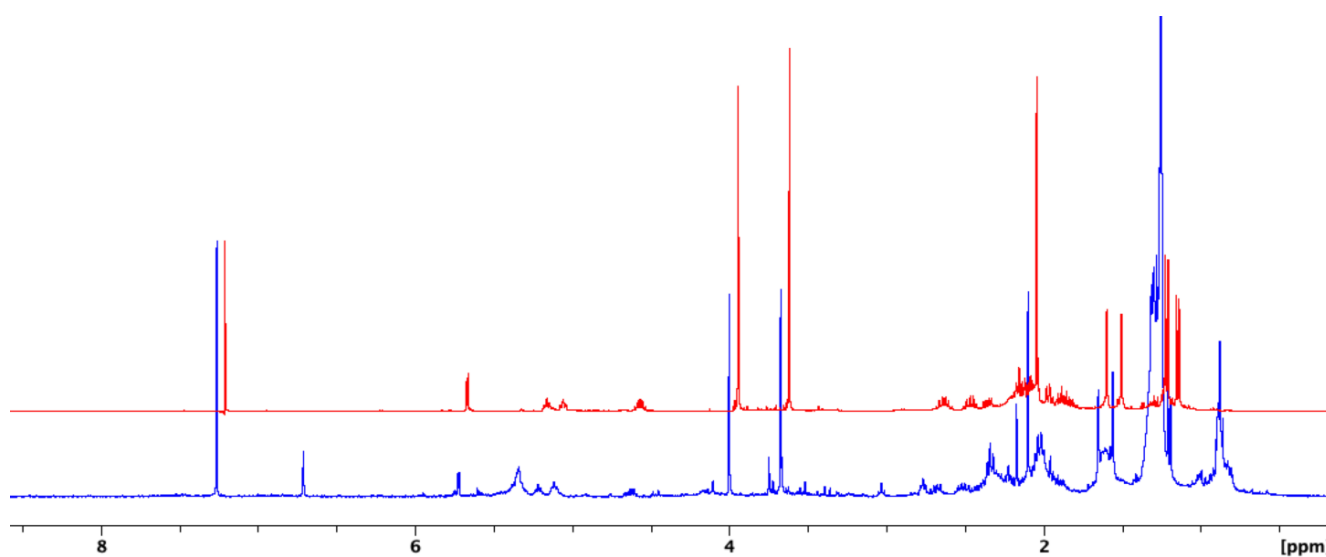


Figure 1. Stacked ^1H NMR spectra of the bioactive Fraction 5 (blue) and the major compound 4-acetylanthroquinol B (red).

To assess the anti-inflammation activity of compound 1 and other phytochemicals in the bioactive Fraction 5, it was further isolated and purified by HPLC. In addition to the identification of 4-acetylanthroquinol B (Figure S2), the phytochemical investigation of Fraction 5 yielded seven compounds, including two anthroquinonols, anthroquinol Y (2) [29] and anthroquinol (3) [30]; a benzenoid, 3-hydroxy-4,5-dimethoxy-2-methylbenzaldehyde (4); two maleimide derivatives, 3-isobutyl-4-(4-methoxyphenyl)-1H-pyrrol-1-ole-2,5-dione (5) and 3-(4-hydroxyphenyl)-4-isobutyl-1H-pyrrole-2,5-dione (6) [31]; and two maleic anhydride derivatives, antrocinnamomin C (7) [32] and antrocinnamomin D (8) [32]. The structures of compounds 1–8 are shown in Figure 2. Their structures were identified by spectral analysis and comparing their data to those reported in the literature. Among them, compounds 4 and 5 were identified as new compounds. Detailed structural elucidation of compounds 4 and 5 was further illustrated by spectral analysis, including MS, IR, and 1D and 2D NMR (Figure S3–S13).

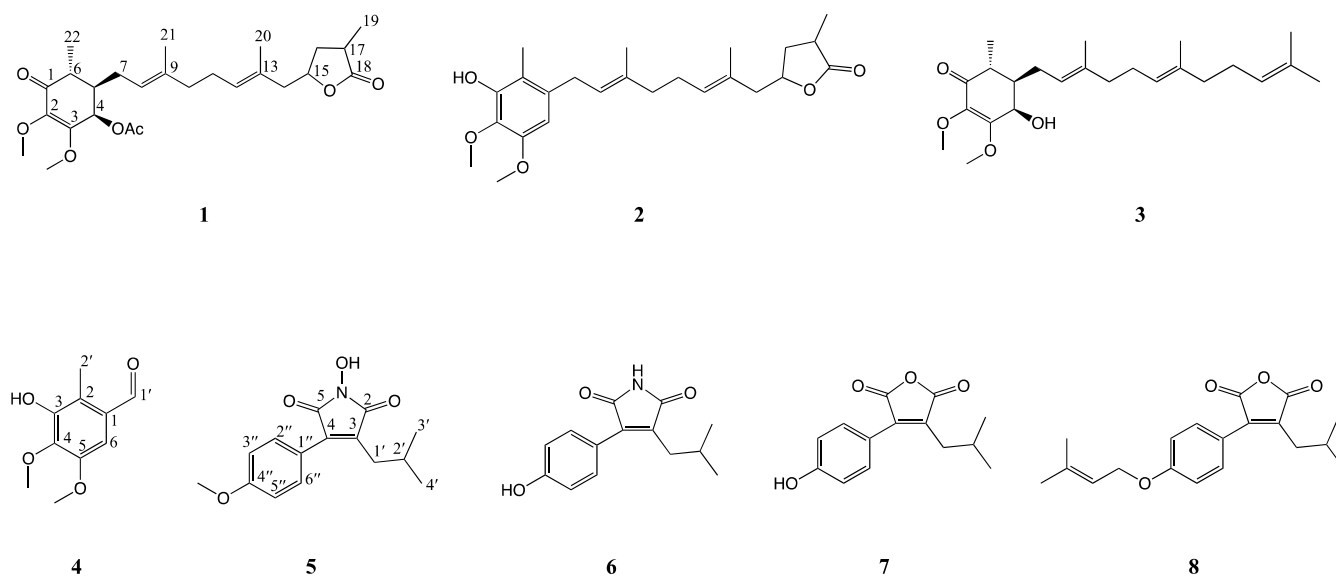


Figure 2. The structures of compounds 1–8 from the mycelium of *A. camphorata*.

Compound 4 was determined to have the molecular formula of $C_{10}H_{12}O_4$ with five degrees of unsaturation according to its HRESIMS peak at m/z 197.0812 $[M + H]^+$. The IR spectrum showed peaks at 3437 (OH), 1670 (aldehyde), and 1593 and 1493 (aromatic) cm^{-1} . The 1H and ^{13}C NMR data revealed the presence of a benzene ring with five substituents—an aldehyde (δ_H 10.25, s), an aryl proton (δ_H 7.02, s, 1H), a hydroxyl proton (δ_H 6.03, s, 1H), two methoxy groups (δ_H 3.99 and 3.90, s, 3H each), and a deshielded methyl group (δ_H 2.51, s, 3H), together with six aromatic carbon signals (δ_C 150.1, 148.0, 140.1, 129.7, 121.4, and 105.0). The methyl signal (δ_H 2.51) resonated at a higher frequency, then indicated that the methyl group is located at the *ortho*-position to the aldehyde group. The relative positions of aryl substituents were confirmed by HMBC correlations (Figure 3) from the methyl protons (δ_H 2.51) to C-1 (δ_C 129.7), C-2 (δ_C 121.4), and C-3 (δ_C 148.0), from the aldehyde proton (H-1', δ_H 10.25) to C-1 (δ_C 129.7) and C-6 (δ_C 105.0), and from the aryl proton (H-6, δ_H 7.02) to C-2 (δ_C 121.4), C-4 (δ_C 140.1), and C-1' (δ_C 191.2). Thus, compound 4 was identified as 3-hydroxy-4,5-dimethoxy-2-methylbenzaldehyde.

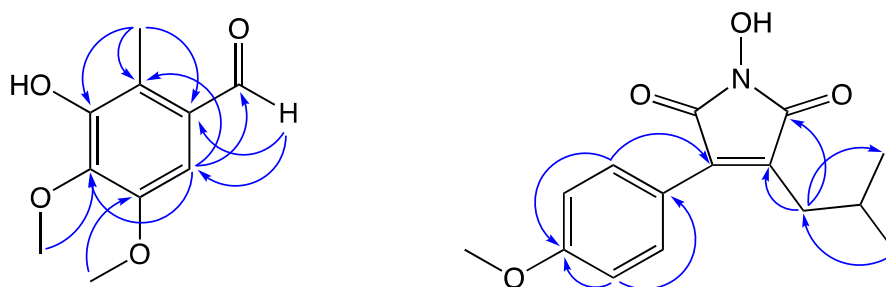


Figure 3. Key HMBC correlations of compounds 4 and 5.

Compound 5 was determined to have the molecular formula of $C_{15}H_{17}NO_4$ with eight degrees of unsaturation according to its HRESIMS peak at m/z 298.1051 $[M + Na]^+$. The IR spectrum showed peaks at 3312 (N-OH), 1776 and 1709 (imide), and 1607 and 1514 (aromatic) cm^{-1} . The 1H NMR data showed the presence of a *para*-substituted aromatic ring (δ_H 7.47 (d, J = 8.6 Hz, 2H) and 6.92 (d, J = 8.6 Hz, 2H)), a hydroxy group (δ_H 5.55, s, 1H), a methoxy group (δ_H 4.00, s, 3H), and an isobutyl group (δ_H 2.51 (d, J = 7.4 Hz, 2H), 2.05 (m, 1H), and 0.90 (d, J = 6.7 Hz, 6H)). The COSY correlations between H-2' and H-1' and two methyl groups further confirmed the presence of the isobutyl group. The ^{13}C NMR data revealed the presence of two carbonyl carbons (δ_C 167.8 and 167.1) and two quaternary

olefinic carbons (δ_C 136.3 and 135.9), which was characteristic of a maleimide moiety. The relative connectivity was further deduced from the HMBC correlations from H-1' (δ_H 2.51) to C-2 (δ_C 167.8) and C-3 (δ_C 136.3), and the HMBC correlations (Figure 3) from H-2'' (δ_H 7.47) to C-4 (δ_C 135.9) and C-4'' (δ_C 157.4). The overall spectroscopic data of compound 5 were similar to those of antrocinamomin B [32]. The only difference is the presence of a methoxy group (δ_C/δ_H 65.9/4.00) in compound 5 instead of a hydroxy group in antrocinamomin B. Thus, compound 5 was identified as 3-isobutyl-4-(4-methoxyphenyl)-1H-pyrrol-1-ol-2,5-dione.

Evaluations for the inhibitory effect on NO production in RAW 264.7 macrophages induced by poly I:C (Table 1) were performed on all isolated compounds. In order to exclude the cytotoxic effect of tested compounds, those were also applied for cell viability assessment. No cytotoxicity was observed (cell viability >90%) when treated with the tested compounds under the half maximal inhibitory concentration. As expected, 4-acetylanthroquinol B (1) shows most potent inhibitory activity against poly I:C induced-NO production in RAW 264.7 cells with an IC_{50} value of 0.57 ± 0.06 μ M. Additionally, two antroquinonols (2 and 3), a benzenoid (4), and two maleimide anhydride derivatives (5 and 6) showed moderate inhibitory activity with the IC_{50} values ranging from 2.96 to 27.14 μ M. However, maleic anhydride derivatives (7 and 8), compared to maleimide derivatives, were found to be not effective in this study. According to the bioactivity results above, together with the relative abundance of different metabolites in the bioactive Fraction 5, 4-acetylanthroquinol B (1) was not only the most abundant compound but the most potent compound against poly I:C-induced NO production in RAW 264.7 cells.

Table 1. Anti-inflammatory activity of compounds 1–8 from *A. camphorata* on NO production in RAW 264.7 macrophages induced by poly I:C.

Compounds	IC_{50} (μ M) ¹
1	0.57 ± 0.06
2	2.96 ± 0.77
3	10.80 ± 1.32
4	10.11 ± 1.76
5	11.30 ± 3.34
6	27.14 ± 4.61
7	>50
8	>50
Indomethacin ²	67.10 ± 2.23

¹ The IC_{50} values were calculated based on the dose–response curves and expressed as mean \pm SD of triplicates. ² Indomethacin was used as a positive control.

Toll-like receptors (TLRs), a class of PPR, play a crucial role in regulating the innate immune system. TLR3 could recognize dsRNA and drive the inflammatory cytokine signaling, such as nuclear factor- κ B (NF- κ B) and mitogen-activated protein (MAP) kinase activation [19]. The preliminary activity of ACM, together with the anti-inflammatory compounds in this study, urges the need for further studies on the TLR3 signaling pathway.

3. Materials and Methods

3.1. General Experimental Procedures

Silica gel (25 μ m) was used for medium-pressure column chromatography (MPLC). Silica gel 60 F254 plates (200 μ m) was used for thin-layer chromatography (TLC). High-performance liquid chromatography (HPLC) was carried out on a KNAUER HPLC system equipped with a refractive index (RI) detector. IR spectra were measured with a Shimadzu IRPrestige-21 Fourier transform infrared (FT-IR) spectrophotometer. High-resolution electrospray mass (HRESIMS) spectra were acquired on a Bruker Daltonics maXis impact ESI-Q-TOF mass spectrophotometer. UV spectra were obtained using a PerkinElmer Lambda 265 UV–Visible spectrophotometer. Nuclear magnetic resonance (NMR) spectra

were measured with a Bruker AVANCE NEO 400 MHz FTNMR spectrometer and a Bruker AVANCE 500 MHz FTNMR spectrophotometer.

3.2. Chemicals

Acetone, dichloromethane, ethyl acetate (EtOAc), *n*-hexane, and deuterated chloroform were obtained from the branch of Merck in Taiwan. Antibiotics (penicillin-streptomycin), Dulbecco's modified Eagle's medium (DMEM), glutamine, and fetal bovine serum (FBS) were purchased from GIBCO (Grand Island, NY, USA). Indomethacin, *N*-(1-naphthyl)ethylenediamine dihydrochloride, polyinosinic-polycytidylic acid (Poly I:C), potassium phosphate-buffered saline (PBS), sodium nitrite, sulphanilamide, and phosphoric acid were obtained from Sigma Chemical Co. (St. Louis, MO, USA).

3.3. Extraction and Isolation

The mycelium of *A. camphorata* (4.1 kg) was extracted with methanol three times at room temperature, and the crude extract was concentrated and applied on MPLC with a linear gradient solvent system of *n*-hexane and EtOAc. Each collected fraction was assigned into ten main fractions based on TLC characterization.

All compounds were obtained from Fraction 5 by semi-preparative HPLC, equipped with a refractive index (RI) detector at a flow rate of 3 mL/min. Fraction 5 was separated by HPLC to yield compound **1** (801.1 mg, *n*-hexane/EtOAc = 2/1, t_R = 18.6 min), re-separated by HPLC (dichloromethane/EtOAc = 6/1) to provide compounds **6** (3.2 mg, t_R = 14.1 min), **7** (2.6 mg, t_R = 6.6 min), and **8** (1.6 mg, t_R = 8.3 min), and further purified by HPLC to give compounds **5** (5.1 mg, *n*-hexane/acetone = 4/1, t_R = 15.2 min), **2** (43.6 mg, *n*-hexane/EtOAc = 4/1, t_R = 23.3 min), **3** (mg, *n*-hexane/EtOAc = 3/2, t_R = 12.5 min), and **4** (7.2 mg, *n*-hexane/EtOAc = 4/1, t_R = 18.1 min).

3-Hydroxy-4,5-dimethoxy-2-methylbenzaldehyde (**4**): Amorphous colorless powder; IR (KBr) ν_{\max} 3437, 3001, 2940, 2866, 1670, 1593, and 1493 cm^{-1} ; UV λ_{\max} (log ϵ , MeOH) 286 (3.81); ^1H and ^{13}C NMR data: Shown in Table 2; HRESIMS m/z 197.0812 [M + H] $^+$.

Table 2. ^{13}C (100 MHz) and ^1H NMR (400 MHz, Chloroform-*d*), and HMBC data of compound **4**.

Position	^{13}C NMR δ_{C}	^1H NMR δ_{H} (Multiplicity)	HMBC
1	129.7		
2	121.4		
3	148.0		
4	140.1		
5	150.1		
6	105.0	7.02 (s)	C-2, C-4, C-5, C-1'
1'	191.2	10.25 (s)	C-1, C-6
2'	9.93	2.51 (s)	C-1, C-2, C-3
3-OH		6.03 (s)	C-2, C-3

3-Isobutyl-4-(4-methoxyphenyl)-1H-pyrrol-1-ol-2,5-dione (**5**): Amorphous colorless powder; IR (KBr) ν_{\max} 3312, 2955, 2924, 2866, 1776, 1709, 1607, 1580, and 1514 cm^{-1} ; UV λ_{\max} (log ϵ , MeOH) 232 (3.63), 284 (3.00), 370 (2.87); ^1H and ^{13}C NMR data: Shown in Table 3; HRESIMS m/z 298.1051 [M + Na] $^+$.

Table 3. ^{13}C (125 MHz) and ^1H NMR (500 MHz, Chloroform-*d*), and HMBC data of compound 5.

Position	^{13}C NMR δ_{C}	^1H NMR δ_{H} (Multiplicity)	HMBC
2	167.8		
3	136.3		
4	135.9		
5	167.1		
1'	33.1	2.51 (d, 7.4)	C-2, C-3, C-3', C-4'
2'	28.2	2.05 (m)	C-1', C-3', C-4'
3', 4'	22.9	0.90 (d, 6.7)	C-1', C-2'
1''	121.2		
2'', 6''	131.5	7.47 (d, 8.6)	C-4, C-3'', C-4'', C-5''
3'', 5''	115.9	6.92 (d, 8.6)	C-1'', C-4''
4''	157.4		
4''-OCH ₃	65.9	4.00 (s)	
OH		5.55 (brs)	

3.4. NO Production and Cell Viability of RAW 264.7 Macrophages Induced by Poly I:C

RAW 264.7 macrophages were cultured in DMEM supplemented with 10% FBS and 1% antibiotics in an incubator with a humidified atmosphere of 5% CO₂ at 37 °C. After being seeded into 96-well plates (5 × 10⁴ cells/well), the cells were incubated overnight and then treated with filtered, tested samples with different concentrations, followed by poly I:C (50 µg/mL). After incubation for 24 h, NO concentration in the culture medium was measured with the Griess reaction and calculated using a standard curve. Each supernatant (100 µL) was reacted with the same volume (100 µL) of Griess reagent (containing 0.05% *N*-(1-naphthyl)ethylenediamine dihydrochloride, 0.5% sulphanilamide, and 2.5% phosphoric acid) for 5 min at room temperature. The absorbance at 540 nm was detected using a microplate reader. The CCK-8 assay was applied for cell viability assessment according to standard protocols. The absorbance at 450 nm was detected using a microplate reader. The experiments were performed in triplicates.

3.5. Statistical Analysis

The results were expressed as mean ± SD of triplicates. Significant differences were examined using a two-tailed unpaired Student's *t* test. *p* values of less than 0.05 were considered statistically significant.

4. Conclusions

In this study, the inhibitory effects of the methanolic extract of the mycelium of *A. camphorata* were assessed on viral infection-associated inflammation using poly I:C-stimulated NO production in a RAW 264.7 mouse macrophage model. Our study provides a precise strategy for screening anti-inflammatory compounds from the mycelium of *A. camphorata* by a combination of bioactivity-guided isolation with an NMR-based identification approach, which led to isolation and identification of eight compounds, including two new compounds 4 and 5. Among them, 4-acetylanthroquinol B (1) was not only the most abundant compound, but the most potent compound in the bioactive Fraction 5 from the mycelium of *A. camphorata*. Thus, it could be a chemical marker for the potential anti-inflammatory agent *A. camphorata* mycelium during viral infection.

Supplementary Materials: The following supporting information can be downloaded at: <https://www.mdpi.com/article/10.3390/molecules27165320/s1>: Figure S1 The effects of the mycelium of *Antrodia camphorata* (ACM) on nitric oxide (NO) production in RAW 264.7 cells induced by polyinosinic–polycytidylic acid (poly I:C). Figure S2 ^1H NMR spectrum of the major compound identified as 4-acetylanthroquinol B in the bioactive fraction 5. Figure S3 MS spectrum of compound 4. Figure S4 ^1H NMR spectrum of compound 4. Figure S5 ^{13}C NMR spectrum of compound 4. Figure S6 HSQC NMR spectrum of compound 4. Figure S7 HMBC NMR spectrum of compound 4. Figure

S8 MS spectrum of compound 5. Figure S9 ^1H NMR spectrum of compound 5. Figure S10 ^{13}C NMR spectrum of compound 5. Figure S11 HSQC NMR spectrum of compound 5. Figure S12 HMBC NMR spectrum of compound 5. Figure S13 COSY NMR spectrum of compound 5.

Author Contributions: Conceptualization, P.-C.T. and W.-P.J.; methodology, P.-C.T. and M.-K.L.; investigation, P.-C.T. and W.-P.J.; resources, M.-K.L. and G.-J.H.; data curation, W.-P.J.; writing—original draft preparation, P.-C.T.; writing—review and editing, Y.-H.K.; supervision—G.-J.H., Y.-J.L. and Y.-H.K.; project administration, Y.-H.K. All authors have read and agreed to the published version of the manuscript.

Funding: This work was financially supported by a China Medical University grant in Taiwan (CMU110-Z-08 and CMU109-AWARD-02) and “Chinese Medicine Research Center, China Medical University” from The Featured Areas Research Center Program within the framework of the Higher Education Sprout Project by the Ministry of Education (MOE) in Taiwan (CMRC-CHM-2-1).

Institutional Review Board Statement: Not applicable.

Informed Consent Statement: Not applicable.

Data Availability Statement: The data presented in this study are available in the supplementary material.

Acknowledgments: Mass spectrometry was performed by the Proteomics Research Core Laboratory, Office of Research & Development at China Medical University, Taichung, Taiwan.

Conflicts of Interest: The authors declare that they have no conflict of interest.

Sample Availability: Samples of the compounds are not available from the authors.

References

1. Roh, J.S.; Sohn, D.H. Damage-associated molecular patterns in inflammatory diseases. *Immune Netw.* **2018**, *18*, e27. [[CrossRef](#)]
2. Lee, J.Y.; Park, W. Anti-inflammatory effect of wogonin on RAW 264.7 mouse macrophages induced with polyinosinic-polycytidylic acid. *Molecules* **2015**, *20*, 6888–6900. [[CrossRef](#)] [[PubMed](#)]
3. Kim, Y.J.; Park, W. Anti-inflammatory effect of quercetin on RAW 264.7 mouse macrophages induced with polyinosinic-polycytidylic acid. *Molecules* **2016**, *21*, 450. [[CrossRef](#)] [[PubMed](#)]
4. Leung, N.H.L. Transmissibility and transmission of respiratory viruses. *Nat. Rev. Microbiol.* **2021**, *19*, 528–545. [[CrossRef](#)] [[PubMed](#)]
5. Ding, Z.; Sun, G.; Zhu, Z. Hesperidin attenuates influenza A virus (H1N1) induced lung injury in rats through its anti-inflammatory effect. *Antivir. Ther.* **2018**, *23*, 611–615. [[CrossRef](#)]
6. Li, Z.; Zhao, J.; Zhou, H.; Li, L.; Ding, Y.; Li, J.; Zhou, B.; Jiang, H.; Zhong, N.; Hu, W.; et al. Cappariloside A shows antiviral and better anti-inflammatory effects against influenza virus via regulating host IFN signaling, in vitro and vivo. *Life Sci.* **2018**, *200*, 115–125. [[CrossRef](#)]
7. Hao, W.; Wang, L.; Li, S. FKBP5 regulates RIG-I-mediated NF- κ B activation and influenza A virus infection. *Viruses* **2020**, *12*, 672. [[CrossRef](#)]
8. Baranwal, M.; Gupta, Y.; Dey, P.; Majaw, S. Antiinflammatory phytochemicals against virus-induced hyperinflammatory responses: Scope, rationale, application, and limitations. *Phytother. Res.* **2021**, *35*, 6148–6169. [[CrossRef](#)]
9. Singla, R.K.; He, X.; Chopra, H.; Tsagkaris, C.; Shen, L.; Kamal, M.A.; Shen, B. Natural products for the prevention and control of the COVID-19 pandemic: Sustainable bioresources. *Front. Pharmacol.* **2021**, *12*, 758159. [[CrossRef](#)]
10. Isidoro, C.; Chang, A.C.F.; Sheen, L.Y. Natural products as a source of novel drugs for treating SARS-CoV2 infection. *J. Tradit. Complement. Med.* **2022**, *12*, 1–5. [[CrossRef](#)]
11. Majnooni, M.B.; Fakhri, S.; Shokoohinia, Y.; Kiyani, N.; Stage, K.; Mohammadi, P.; Gravandi, M.M.; Farzaei, M.H.; Echeverría, J. Phytochemicals: Potential Therapeutic interventions against coronavirus-associated lung injury. *Front. Pharmacol.* **2020**, *11*, 588467. [[CrossRef](#)]
12. Geethangili, M.; Tzeng, Y.M. Review of pharmacological effects of *Antrodia camphorata* and its bioactive compounds. *Evid. Based Complement. Altern. Med.* **2011**, *2011*, 212641. [[CrossRef](#)] [[PubMed](#)]
13. Ganesan, N.; Baskaran, R.; Velmurugan, B.K.; Thanh, N.C. *Antrodia cinnamomea*—An updated minireview of its bioactive components and biological activity. *J. Food Biochem.* **2019**, *43*, e12936. [[CrossRef](#)] [[PubMed](#)]
14. Senthil Kumar, K.J.; Gokila Vani, M.; Chen, C.Y.; Hsiao, W.W.; Li, J.; Lin, Z.X.; Chu, F.H.; Yen, G.C.; Wang, S.Y. A mechanistic and empirical review of antcins, a new class of phytosterols of formosan fungi origin. *J. Food Drug Anal.* **2020**, *28*, 38–59. [[CrossRef](#)] [[PubMed](#)]
15. Kuang, Y.; Li, B.; Qiao, X.; Ye, M. Terpenoids from the medicinal mushroom *Antrodia camphorata*: Chemistry and medicinal potential. *Nat. Prod. Rep.* **2021**, *38*, 83–102. [[CrossRef](#)]

16. Senthil Kumar, K.J.; Gokila Vani, M.; Hsieh, H.W.; Lin, C.C.; Wang, S.Y. Anticins from *Antrodia cinnamomea* and *Antrodia salmonea* inhibit angiotensin-converting enzyme 2 (ACE2) in epithelial cells: Can be potential candidates for the development of SARS-CoV-2 prophylactic agents. *Plants* **2021**, *10*, 1736. [[CrossRef](#)]
17. Graziani, V.; Scognamiglio, M.; Belli, V.; Esposito, A.; D'Abrosca, B.; Chambery, A.; Russo, R.; Panella, M.; Russo, A.; Ciardiello, F.; et al. Metabolomic approach for a rapid identification of natural products with cytotoxic activity against human colorectal cancer cells. *Sci. Rep.* **2018**, *8*, 5309. [[CrossRef](#)]
18. Tu, P.C.; Chan, C.J.; Liu, Y.C.; Kuo, Y.H.; Lin, M.K.; Lee, M.S. Bioactivity-guided fractionation and NMR-based identification of the immunomodulatory isoflavone from the roots of *Uraria crinita* (L.) Desv. ex DC. *Foods* **2019**, *8*, 543. [[CrossRef](#)]
19. Kim, H.J.; Kim, Y.J.; Park, W. Berberine modulates hyper-inflammation in mouse macrophages stimulated with polyinosinic-polycytidylic acid via calcium-CHOP/STAT pathway. *Sci. Rep.* **2021**, *11*, 11298. [[CrossRef](#)]
20. Gao, X.; Chen, P.K.S.; Lui, G.C.Y.; Hui, D.S.C.; Chu, I.M.T.; Sun, X.; Tsang, M.S.M.; Chan, B.C.L.; Lam, C.W.; Wong, C.K. Interleukin-38 ameliorates poly(I:C) induced lung inflammation: Therapeutic implications in respiratory viral infections. *Cell Death Dis.* **2021**, *12*, 53. [[CrossRef](#)]
21. Kim, Y.-J.; Kim, H.-J.; Lee, J.Y.; Kim, D.-H.; Kang, M.S.; Park, W. Anti-inflammatory effect of baicalein on polyinosinic-polycytidylic acid-induced RAW 264.7 mouse macrophages. *Viruses* **2018**, *10*, 224. [[CrossRef](#)]
22. Lin, Y.-W.; Pan, J.-H.; Liu, R.H.; Kuo, Y.-H.; Sheen, L.-Y.; Chiang, B.-H. The 4-acetylanthroquinol B isolated from mycelium of *Antrodia cinnamomea* inhibits proliferation of hepatoma cells. *J. Sci. Food Agric.* **2010**, *90*, 1739–1744. [[CrossRef](#)] [[PubMed](#)]
23. Li, T.-Y.; Chiang, B.-H. 4-Acetylanthroquinol B from *Antrodia cinnamomea* enhances immune T function of dendritic cells against liver cancer stem cells. *Biomed. Pharmacother.* **2019**, *109*, 2262–2269. [[CrossRef](#)] [[PubMed](#)]
24. Yen, I.-C.; Tu, Q.-W.; Chang, T.-S.; Lin, P.-H.; Li, Y.-F.; Li, S.-Y. 4-Acetylanthroquinol B ameliorates nonalcoholic steatohepatitis by suppression of ER stress and NLRP3 inflammasome activation. *Biomed. Pharmacother.* **2021**, *138*, 111504. [[CrossRef](#)] [[PubMed](#)]
25. Chang, C.-H.; Hsu, C.-C.; Lee, A.-S.; Wang, S.-W.; Lin, K.-T.; Chang, W.-L.; Peng, H.-C.; Huang, W.-C.; Chung, C.-H. 4-Acetylanthroquinol B inhibits lipopolysaccharide-induced cytokine release and alleviates sepsis through of MAPK and NFκB suppression. *BMC Complement. Altern. Med.* **2018**, *18*, 108. [[CrossRef](#)] [[PubMed](#)]
26. Liu, M.; Bamodu, O.A.; Huang, W.C.; Zucha, M.A.; Lin, Y.-K.; Wu, A.T.H.; Huang, C.-C.; Lee, W.-H.; Yuan, C.-C.; Hsiao, M.; et al. 4-Acetylanthroquinol B suppresses autophagic flux and improves cisplatin sensitivity in highly aggressive epithelial cancer through the PI3K/Akt/mTOR/p70S6K signaling pathway. *Toxicol. Appl. Pharmacol.* **2017**, *325*, 48–60. [[CrossRef](#)] [[PubMed](#)]
27. Satriyo, P.B.; Su, C.M.; Ong, J.R.; Huang, W.-C.; Fong, I.-H.; Lin, C.-C.; Aryandono, T.; Haryana, S.M.; Deng, L.; Huang, C.-C.; et al. 4-Acetylanthroquinol B induced DNA damage response signaling and apoptosis via suppressing CDK2/CDK4 expression in triple negative breast cancer cells. *Toxicol. Appl. Pharmacol.* **2021**, *422*, 115493. [[CrossRef](#)]
28. Huang, T.-F.; Wang, S.-W.; Lai, Y.-W.; Liu, S.-C.; Chen, Y.-J.; Hsueh, T.Y.; Lin, C.-C.; Lin, C.-H.; Chung, C.-H. 4-Acetylanthroquinol B suppresses prostate cancer growth and angiogenesis via VEGF/PI3K/ERK/mTOR-dependent signaling pathway in subcutaneous xenograft and in vivo angiogenesis models. *Int. J. Mol. Sci.* **2022**, *23*, 1446. [[CrossRef](#)]
29. Li, B.; Lu, Y.-Y.; Lo, J.-Y.; Qiao, X.; Ye, M. Chemical constituents from the dish-cultured *Antrodia camphorata* and their cytotoxic activities. *J. Asian Nat. Prod. Res.* **2021**, *23*, 666–674. [[CrossRef](#)]
30. Lee, T.-H.; Lee, C.-K.; Tsou, W.-L.; Liu, S.-Y.; Kuo, M.-T.; Wen, W.-C. A new cytotoxic agent from solid-state fermented mycelium of *Antrodia camphorata*. *Planta Med.* **2007**, *73*, 1412–1415. [[CrossRef](#)]
31. Chien, S.-C.; Chen, M.-L.; Kuo, H.-T.; Tsai, Y.-C.; Lin, B.-F.; Kuo, Y.-H. Anti-inflammatory activities of new succinic and maleic derivatives from the fruiting body of *Antrodia camphorata*. *J. Agric. Food Chem.* **2008**, *56*, 7017–7022. [[CrossRef](#)]
32. Wu, M.-D.; Cheng, M.J.; Wang, B.C.; Yech, Y.J.; Lai, J.T.; Kuo, Y.-H.; Yuan, K.-F.; Chen, I.S. Maleimide and maleic anhydride derivatives from the mycelia of *Antrodia cinnamomea* and their nitric oxide inhibitory activities in macrophages. *J. Nat. Prod.* **2008**, *71*, 1258–1261. [[CrossRef](#)] [[PubMed](#)]